DINAME 2017 - Proceedings of the XVII International Symposium on Dynamic Problems of Mechanics
M. F. Wu, R. U. Mendes, K. L. Cavalca, ABCM, São Sebastião, SP, Brazil, March 5-10, 2017

Vibration Control of a Journal-Bearing Supported Rotor Using Gain-Scheduled Controller via LMI

Matheus Freire Wu[1], **Ricardo Ugliara Mendes**[2] **and Katia Lucchesi Cavalca**[3]

[1, 2, 3] Laboratory of Rotating Machinery, Faculty of Mechanical Engineering, University of Campinas, 200 Mendeleiev Street, 13083-970 Campinas, São Paulo, Brazil
[1] matheusfw@fem.unicamp.br
[2] rumqld@gmail.com
[3] katia@fem.unicamp.br

Abstract: Rotating machinery concepts are present in several modern industrial applications. Typically, the main obstacles to achieve higher efficiency, speed and reliability are phenomena that cause vibration. An interesting option for rotor support are hydrodynamic bearings, which offer low friction, high damping, and a good ratio between load and operational speed. However, there is a downside, the oil-whip excites the system and sets a threshold to rotational speed due to high vibration levels, known as fluid-induced instability. This behavior can be described by a nonlinear variation of the system's model parameters (damping and stiffness) according to the rotational speed. This paper aims to determine an active control law that allows surpassing the instability rotational speed threshold, via a magnetic actuator. For this matter, a two-stage linear matrix inequalities (LMI) approach is used to determine an output gain matrix, dependant on the rotational speed, able to stabilize the oil-whip and reduce the vibration levels at the critical speed. The attained performance is analyzed by means of numerical simulations, and then compared to μ-synthesis and H_∞ controllers.

Keywords: rotating machinery, oil-whip, LMI, gain-scheduled control

INTRODUCTION

In industrial and power generation applications most of the dynamic equipments are composed by rotating machinery components. It is clear that, frequently, problems concerning efficiency, lifetime and safety are somehow related to the system's vibration levels. Active vibration control methods arise as an interesting alternative to work out those issues. One of the major obstacles to implement active control techniques concerning rotating machinery are the system's parametrical variations according to the operational speed. This phenomenon occurs mainly due to gyroscopic effect or behavior associated to components such as hydrodynamic bearings. Even though hydrodynamic bearings provide several attractive characteristics for practical application, for instance, high load and damping capability, low frictional coefficient and extended lifetime, they present a downside, the oil-whirl and oil-whip effects. These are auto-induced excitations that can lead the system to instability at rotations close to twice the critical speed establishing a threshold. In this context, one can say that there are two main applicable control theory approaches: robust and adaptive. The first consists on obtaining a single controller that assures stability for any possible system variation. And the former on determining a control function that depends on the system's varying parameters, aiming to attain optimum performance for each operational condition.

Many studies in the area of active rotor control are regarding magnetic levitation utilizing active magnetic bearings (AMB). One of the earliest successful applications was achieved by Fujita et al. (1993) utilizing H_∞ control techniques. Nonami and Ito (1996) compared H_∞ and μ-synthesis performance and robustness aiming to keep levitation and attenuate the vibration of a system under different load conditions. Fittro and Knospe (2002) compared PID, H_∞ and μ-synthesis controllers seeking to maintain levitation and reduce vibration at the middle of a flexible shaft with the actuators placed in the far ends. The authors mentioned that the μ-synthesis controller presented unstable poles. The unstable AMB controllers issue was later investigated by Balini et al. (2011), who also proposed a switching start-up solution. A good overview about AMB systems can be found in Maslen (2009). Riemann et al. (2013a and 2013b) presented a research with a more similar outline to what is addressed in this paper, the magnetic actuator is applied only for stabilization and vibration attenuation purposes, while the shaft is actually supported by journal bearings.

On the topic of adaptive control, one of the first reports of AMB application was given by Matsumura et al. (1996), concerned about robustness regarding gyroscopic effect. In this work, a set of H_∞ controller was arranged as a gain-scheduled function of the rotational speed. The problem with the approach taken by Matsumura et al. (1996) is the lack of stability certification. To deal with this issue, Wu (2001) designed and simulated the response of an output-feedback linear parameter varying (LPV) controller for a flexible AMB system based on Lyapunov stability. Lu et al. (2006)

successfully implemented a LPV H_∞ state-feedback controller, also based on Lyapunov stability. In Siqueira et al. (2012) a successfully implementation of an LPV H_∞ output-feedback is reported to greatly reduce vibration level of a hydrodynamic rotor bearing system. However the applied control formulation was dependant on the system space-state matrix and, under uncertain condition, may present performance issues. A study comparing, through simulations, the performance and stability of H_∞, μ-Synthesis and H_∞ state-feedback LPV applied to hydrodynamic bearing systems can be found in Wu et al. (2015a).

This paper aims to show, by computational simulations, the potential of gain-scheduled output-feedback controller in surpassing the fluid-induced instability and attenuating the vibration at critical speed. The control technique applied was described in Agulhari et al. (2012a), and consists in a two stage design based on linear matrices inequalities (LMI) Lyapunov stability, which provides stability and performance guarantee. The first stage is to determine a state-feedback stabilizable control gain. The second stage is the proper calculation of the output-feedback gain, which utilizes the first stage as an input to formulate a linear optimization problem. For comparison purposes, the attained controller is also compared to H_∞ and μ-Synthesis designs, Wu et al. (2015b). Although it is not explored in this current study, this approach can deal with sources of unmonitored parametrical uncertainties offering a robust solution if required.

MATERIALS AND METHOD

Rotor Model

The rotor utilized in this paper consists in a steel (SAE 1030) shaft of 12mm diameter and 800mm length, supported by two hydrodynamic bearings of 30mm diameter, 20mm length and radial clearance of 90μm, symmetrically placed 600mm away from each other, lubricated by ISO VG 32 oil. A steel disc of 95mm diameter and 47,5mm length is placed in the middle of the shaft. The control force actuates over the system through a steel journal of 40mm diameter and 80mm length, placed with its center 102mm away from the second bearing. With this configuration, the rotor presents its first critical speed at approximately 23Hz, and its instability at about 47Hz.

The sensor availability considers access to rotational speed, and horizontal and vertical displacements of the bearings. Although one of the objectives of the control is to attenuate the vibration level of the disc, in real applications its displacement measurement is usually not possible. Hence, the control is expected to operate with feedback of rotational speed and bearings displacement, while seeking to attenuate the vibration of the disc.

The system was represented using finite element model (FEM) based on the formulation from Nelson and MacVaugh (1976). The shaft is divided into 21 nodes, according to Figure 1, each node presents 4 degrees of freedom (DOF) (2 translations and 2 rotations), resulting in 84 degrees of freedom. The bearings damping and stiffness coefficients were modeled by Machado and Cavalca (2009). Concatenating mass, stiffness, damping and gyroscopic matrices of the elements, and properly adding the equivalent bearings coefficients, it was obtained the respective global matrices $\mathbf{M_{fem}}$, $\mathbf{K_{fem}}$, $\mathbf{C_{fem}}$ and $\mathbf{G_{fem}}$, utilized to formulate the equation of motion Eq. (1). This model was previously validated in a test rig by Mendes et al. (2013) and Mendes (2016).

$$\mathbf{M_{fem}}\ddot{\mathbf{q}} + (\mathbf{C_{fem}}(\Omega) + \Omega\mathbf{G_{fem}})\dot{\mathbf{q}} + \mathbf{K_{fem}}(\Omega)\mathbf{q} = \mathbf{F_e} \tag{1}$$

$\mathbf{q}$, $\dot{\mathbf{q}}$, $\ddot{\mathbf{q}}$: nodes displacements, speeds and accelerations.
$\mathbf{F_e}$: exogenous forces (unbalance and control).
Ω: rotational speed.

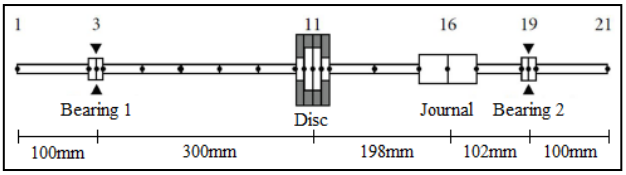

Figure 1 – Rotor scheme, adapted from Mendes et al. (2013).

Model reduction and polynomial approximation

In order to apply the proposed control technique, the problem has to be properly formulated. The original system space-state representation has 168 states, which can be considered an elevated order for solving LMI problems. To tackle this issue, the Guyan reduction method was applied (Eq. (2)), where $\mathbf{T}$ is the transformation matrix and $\mathbf{T'}$ is the transpose of $\mathbf{T}$), Guyan (1965). Therefore, a reduced model of the rotor considers only the key nodes for the control: bearings, disc and actuator journal (3, 11, 16 and 19), totalizing 16 DOF.

$$\mathbf{Mr_{fem}} = \mathbf{T'M_{fem}T} \quad \mathbf{Cr_{fem}} = \mathbf{T'C_{fem}T} \quad \mathbf{Kr_{fem}} = \mathbf{T'K_{fem}T} \quad \mathbf{Gr_{fem}} = \mathbf{T'G_{fem}T} \tag{2}$$

It is important to remark the dependency of Eq. (1) on the rotational speed Ω, not only because of the gyroscopic matrix, but also due to the nonlinear behavior of the hydrodynamic bearings coefficients of stiffness and damping. In this work the considered operational speed slowly varies from 10Hz to 55Hz, covering the range from below to above the instability speed and including the first critical speed. This gain-scheduled control strategy requires expressing the system's parametrical variations as polynomials. For this reason, it was necessary to find a polynomial fit, in this case, using the least squares approximation to a second order polynomial for the bearings variation (terms with subscripts $_{\mathbf{br0}}$, $_{\mathbf{br1}}$ and $_{\mathbf{br2}}$). The bearings coefficients matrices were, then, added to the respective FEM nodes obtaining $\mathbf{Crr_{fem}}$ and $\mathbf{Krr_{fem}}$ matrices, Eq. (3). As a result, the system space-state is described by Eq. (4).

$$\begin{cases} \mathbf{Krr_{fem}}(\Omega) = \mathbf{Kr_{fem}} + \mathbf{K_{br0}} + \mathbf{K_{br1}}\Omega + \mathbf{K_{br2}}\Omega^2 \\ \mathbf{Crr}_{\text{fem}}(\Omega) = \mathbf{Cr_{fem}} + \mathbf{C_{br0}} + \mathbf{C_{br1}}\Omega + \mathbf{C_{br2}}\Omega^2 \end{cases} \tag{3}$$

$$\begin{cases} \dot{\mathbf{x}} = \mathbf{A}(\Omega)\mathbf{x} + \mathbf{B_1}\mathbf{w} + \mathbf{B_2}\mathbf{u} \\ \mathbf{z} = \mathbf{C_1}\mathbf{x} + \mathbf{D_{11}}\mathbf{w} + \mathbf{D_{12}}\mathbf{u} \\ \mathbf{y} = \mathbf{C_2}\mathbf{x} + \mathbf{D_{21}}\mathbf{w} + \mathbf{D_{22}}\mathbf{u} \end{cases} \tag{4}$$

Where,

$$\mathbf{A}(\Omega) = \mathbf{A_1} + \mathbf{A_2}\Omega + \mathbf{A_3}\Omega^2 = \begin{bmatrix} \mathbf{0} & \mathbf{I} \\ -\mathbf{Mr_{fem}}^{-1}\mathbf{Krr_{fem0}} & -\mathbf{Mr_{fem}}^{-1}\mathbf{Crr_{fem0}} \end{bmatrix} + \begin{bmatrix} \mathbf{0} & \mathbf{0} \\ -\mathbf{Mr_{fem}}^{-1}\mathbf{Krr_{fem1}} & -\mathbf{Mr_{fem}}^{-1}(\mathbf{Crr_{fem1}} + \mathbf{Gr_{fem}}) \end{bmatrix}\Omega + \begin{bmatrix} \mathbf{0} & \mathbf{0} \\ -\mathbf{Mr_{fem}}^{-1}\mathbf{Krr_{fem2}} & -\mathbf{Mr_{fem}}^{-1}\mathbf{Crr_{fem2}} \end{bmatrix}\Omega^2$$

x, **z**, **y**, **w** and **u**: state, performance, sensor reading, unbalance force and actuator force vectors, respectively.
A, $\mathbf{B_1}$, $\mathbf{B_2}$: Plant states, unbalance force input and control force input matrices, respectively.
$\mathbf{C_1}$, $\mathbf{D_{11}}$, $\mathbf{D_{12}}$: Performance states, unbalance force input, control signal matrices, respectively.
$\mathbf{C_2}$, $\mathbf{D_{21}}$, $\mathbf{D_{22}}$: Output (sensor) states, unbalance force input, control signal matrices, respectively.

To simplify the control formulation, an interesting step is to normalize the varying parameter (Ω), describing it as a function of a unitary simplex (Δ), Eq. (5) and (6).

$$\alpha \in \Delta_2 \Leftrightarrow \sum_{n=1}^{2} \alpha_n = 1, \alpha_n \geq 0 \tag{5}$$

$$\Omega = \alpha_1(b-a) + a \tag{6}$$

a, b: minimum and maximum rotational frequency (10Hz and 55Hz), respectively.

Substituting Eq. (6) in the state-space matrix **A**(Ω) results in Eq. (7).

$$\begin{aligned} &\mathbf{A}(\Omega) = \mathbf{A}(\alpha) = \mathbf{Ap_1} + \mathbf{Ap_2}\alpha_1 + \mathbf{Ap_3}{\alpha_1}^2 = \\ &\left[\mathbf{A_1} + \mathbf{A_2}a + \mathbf{A_3}a^2\right] + \left[\mathbf{A_2}(b-a) + \mathbf{A_3}2a(b-a)\right]\alpha_1 + \left[\mathbf{A_3}(b-a)^2\right]{\alpha_1}^2 \end{aligned} \tag{7}$$

Homogenizing Eq. (7), that is, multiplying the terms of degree smaller than 2 by $(\alpha_1 + \alpha_2)^n = 1^n$ in order to achieve monomials of the same degree of dependency on α, the formulation provides a less conservative control, Eq. (8).

$$\begin{aligned} &\mathbf{A}(\alpha) = \mathbf{Ap_I}{\alpha_1}^2 + \mathbf{Ap_{II}}\alpha_1\alpha_2 + \mathbf{Ap_{III}}{\alpha_2}^2 = \\ &\left[\mathbf{Ap_1} + \mathbf{Ap_2} + \mathbf{Ap_3}\right]{\alpha_1}^2 + \left[2\mathbf{Ap_1} + \mathbf{Ap_2}\right]\alpha_1\alpha_2 + \left[\mathbf{Ap_1}\right]{\alpha_2}^2 \end{aligned} \tag{8}$$

Quadratic Lyapunov stability

The stability analysis of a system is essential to a project. In current control theory, Lyapunov stability is one of the most important concepts. Several Lyapunov functions structures can be found in literature. This paper uses the quadratic form for uncertain systems, Theorem 1, proposed by Ramos and Peres (2001), to verify the system stability and also to synthesize the gain-scheduled controllers.

Theorem 1: A time invariant uncertain system with space-state matrix $\mathbf{A}(\alpha)$ described by Eq. (9) is stable if there is a Lyapunov matrix $\mathbf{P}(\alpha)$, Eq. (10), that satisfies Eq. (11) conditions.

$$\mathbf{A}(\alpha)=\sum_{i=0}^{n}\mathbf{A}_{i+1}\alpha_1{}^{i}\alpha_2{}^{n-i},\ \alpha\in\Delta_2 \tag{9}$$

$$\mathbf{P}(\alpha)=\sum_{i=0}^{m}\mathbf{P}_{i+1}\alpha_1{}^{i}\alpha_2{}^{m-i},\ \alpha\in\Delta_2 \tag{10}$$

$$\begin{cases}\mathbf{P}(\alpha)>0\\ \mathbf{A}(\alpha)'\mathbf{P}(\alpha)+\mathbf{P}(\alpha)\mathbf{A}(\alpha)<0\end{cases} \tag{11}$$

Since $\alpha\geq 0$ and the conditions in Eq. (11) are polynomials, as a relaxation process, they can be decomposed in several linear inequalities for each monomial term according to Eq. (12). For clarification, their respective α exponents are depicted.

$$\begin{cases}\mathbf{P}_{i+1}>0, i\in[0,m]\rightarrow\alpha_1{}^{i}\alpha_2{}^{m-i}\\ \left(\mathbf{A}_1'\mathbf{P}_{m+1}+\mathbf{P}_{m+1}\mathbf{A}_1\right)<0\rightarrow\alpha_1{}^{0}\alpha_2{}^{n+m}\\ \left(\mathbf{A}_1'\mathbf{P}_m+\mathbf{P}_m\mathbf{A}_1+\mathbf{A}_2'\mathbf{P}_{m+1}+\mathbf{P}_{m+1}\mathbf{A}_2\right)<0\rightarrow\alpha_1{}^{1}\alpha_2{}^{n+m-1}\\ \vdots\\ \left(\mathbf{A}_{n+1}'\mathbf{P}_1+\mathbf{P}_1\mathbf{A}_{n+1}\right)<0\rightarrow\alpha_1{}^{n+m}\alpha_2{}^{0}\end{cases} \tag{12}$$

Gain-Scheduled output-feedback H_∞ control

Generally state-feedback controllers are easier to design and offer the better performance than the output-feedback ones. However, in most practical applications, it is impossible to provide the system's full state vector condition. An alternative is to utilize estimators and observers, but often the well-known techniques require a precise model of the system and thus may face problems due to parametrical uncertainties. To deal with these difficulties, this work applies the two-stage method described in Agulhari et al.(2012a). Based on Lyapunov stability condition and LMI formulation, this output-feedback controller allows to take into account monitored and unmonitored parametrical variations. Moreover, the resulting controller is a matrix polynomial with significant small order, which can be a great advantage for real time applications.

From this point on, any parameter dependant matrices, expressed as $\mathbf{X}(\alpha)$, will be assumed to be an homogeneous matrix polynomial of arbitrary degree, with the same structure as in Eq. (8). Considering the system described by Eqs. (4) and (8), where $\mathbf{x},\dot{\mathbf{x}}\in\Re^n$, $\mathbf{w}\in\Re^i$, $\mathbf{u}\in\Re^c$, $\mathbf{y}\in\Re^o$ and $\mathbf{D_{11}},\mathbf{D_{21}},\mathbf{D_{22}}=\mathbf{0}$, the objective is to find a control gain $\mathbf{L}(\alpha)\in\Re^{c,o}$ that guarantee the stability and minimize the H_∞ norm, reducing the peak response at the critical speed, of the closed loop system (subscripts $_{\mathbf{CL}}$), described by Eq. (13) and Figure 2. It is important to stress that the original problem is not convex, and the methodology presented by Agulhari et al.(2012a) requires some linearization in order to formulate the problem by means of LMI, resulting in sufficient but not necessary conditions. Hence, even if no controller is found by this method, it does not mean there isn't a solution, and also, if there is a solution, that may not be the optimum one.

$$\begin{cases}\dot{\mathbf{x}}=\left(\mathbf{A}(\alpha)+\mathbf{B_2}\mathbf{L}(\alpha)\mathbf{C_2}\right)\mathrm{x}+\mathbf{B_1}\mathbf{w}\\ \mathbf{z}=\left(\mathbf{C_1}+\mathbf{D_{12}}\mathbf{L}(\alpha)\mathbf{C_2}\right)\mathbf{x}\end{cases}=\begin{cases}\dot{\mathbf{x}}=\mathbf{A_{CL}}(\alpha)\mathrm{x}+\mathbf{B_{CL}}\mathbf{w}\\ \mathbf{z}=\mathbf{C_{CL}}(\alpha)\mathbf{x}\end{cases} \tag{13}$$

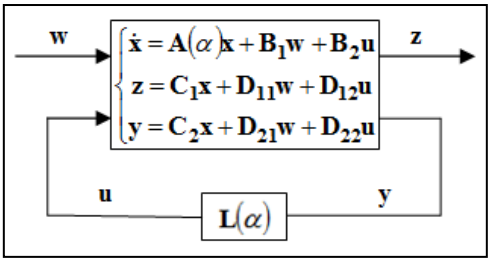

Figure 2 – Control diagram.

The first stage is to find an arbitrary state-feedback control gain $\mathbf{K}(\alpha) \in \Re^{c,n}$ that stabilizes the system from Eq.(14). The resultant gain will have some implications over the final result; however, it is difficult to predict its influence on the second stage performance and feasibility. For this reason, the most important aspect in the first stage is to utilize a method that can provide multiple solutions, therefore several tests possibilities for the second stage. In this case it is applied the same technique utilized in Agulhari et al.(2012a), following Theorem 2, which allows to obtain different $\mathbf{K}(\alpha)$ by choosing different values for the slack variable ξ.

$$\dot{\mathbf{x}} = (\mathbf{A}(\alpha) + \mathbf{B_2}\mathbf{K}(\alpha))\mathrm{x} + \mathbf{B_1}\mathbf{w} \tag{14}$$

Theorem 2: A state-feedback gain $\mathbf{K}(\alpha)$ that stabilizes the system from Eq. (4) exists, if there are $\mathbf{W}(\alpha) = \mathbf{W}'(\alpha) > \mathbf{0} \in \Re^{n,n}$, $\mathbf{X} \in \Re^{n,n}$ and $\mathbf{Z}(\alpha) \in \Re^{i,n}$ for a given $\xi > 0 \in \Re$, which fulfill the LMI from Eq. (15).

$$\begin{bmatrix} \mathbf{A}(\alpha)\mathbf{X} + \mathbf{X}'\mathbf{A}(\alpha)' + \mathbf{B_2}\mathbf{Z}(\alpha) + \mathbf{Z}(\alpha)'\mathbf{B_2}' & \mathbf{W}(\alpha) - \mathbf{X}' + \xi\mathbf{A}(\alpha)\mathbf{X} + \xi\mathbf{B_2}\mathbf{Z}(\alpha) \\ * & -\xi\mathbf{X} - \xi\mathbf{X}' \end{bmatrix} < \mathbf{0} \tag{15}$$

Where,

$$\mathbf{K}(\alpha) = \mathbf{Z}(\alpha)\mathbf{X}^{-1}$$

*****: Transpose of the triangular matrix.

Proof: The theorem proof utilizes an application of the Finsler Theorem, Skelton et al. (1998), which results in the conditions given by Eq. (16).

$$\begin{cases} -2\xi\mathbf{W}(\alpha) < \mathbf{0} \\ \left(\mathbf{A}(\alpha) + \mathbf{B_2}\mathbf{Z}(\alpha)\mathbf{X}^{-1}\right)\mathbf{W}(\alpha) + \mathbf{W}(\alpha)\left(\mathbf{A}(\alpha) + \mathbf{B_2}\mathbf{Z}(\alpha)\mathbf{X}^{-1}\right)' < \mathbf{0} \end{cases} \tag{16}$$

The first condition of Eq. (16) is always true since $\mathbf{W}, \xi > 0$. The second one describes the state-feedback closed-loop stability condition with slack variable, see Bernussou et al. (1989).

■

In Theorem 2, it is possible to notice that one can easily apply less conservative relaxations increasing the polynomial degree of the variables $\mathbf{W}(\alpha)$ and $\mathbf{Z}(\alpha)$ structures or applying Polya relaxation method, Scherer (2006). However, it is important to bear in mind that applying these relaxations results in higher computational effort. The same logic can be applied to the second stage, which follows Theorem 3.

Theorem 3: There exists an output-feedback control gain $\mathbf{L}(\alpha)$ that stabilizes the system from Eq. (13) and minimizes it's infinity norm if there are $\mathbf{P}(\alpha) = \mathbf{P}(\alpha)' > \mathbf{0} \in \Re^{n,n}$, $\mathbf{K}(\alpha) \in \Re^{c,n}$, $\mathbf{F}(\alpha) \in \Re^{n,n}$, $\mathbf{G}(\alpha) \in \Re^{n,n}$, $\mathbf{H} \in \Re^{c,c}$, $\mathbf{J}(\alpha) \in \Re^{c,o}$ and $\mu = \gamma^2 > 0 \in \Re$ that fulfill the LMI problem in Eq. (17).

$$\inf\left(\mu : \begin{bmatrix} \boldsymbol{\Psi}_{11} & \boldsymbol{\Psi}_{12} & \boldsymbol{\Psi}_{13} & \boldsymbol{\Psi}_{14} & \boldsymbol{\Psi}_{15} \\ & -\mathbf{G}(\alpha) - \mathbf{G}(\alpha)' & \mathbf{G}(\alpha)\mathbf{B}_1 & \mathbf{0} & \mathbf{G}(\alpha)\mathbf{B}_2 \\ & & -\mathbf{I} & \mathbf{0} & \mathbf{0} \\ & & & -\mu\mathbf{I} & \mathbf{0} \\ * & & & & -\mathbf{H} - \mathbf{H}' \end{bmatrix} < \mathbf{0}\right) \tag{17}$$

Where,

$$\mathbf{L}(\alpha) = \mathbf{H}^{-1}\mathbf{J}(\alpha)$$

$$\boldsymbol{\Psi}_{11} = \mathbf{A}(\alpha)'\mathbf{F}(\alpha)' + \mathbf{F}(\alpha)\mathbf{A}(\alpha) + \mathbf{K}(\alpha)'\mathbf{B}_2'\mathbf{F}(\alpha)' + \mathbf{F}(\alpha)\mathbf{B}_2\mathbf{K}(\alpha)$$

$$\boldsymbol{\Psi}_{12} = \mathbf{P}(\alpha) - \mathbf{F}(\alpha) + \mathbf{A}(\alpha)'\mathbf{G}(\alpha)' + \mathbf{K}(\alpha)'\mathbf{B}_2'\mathbf{G}(\alpha)'$$

$$\boldsymbol{\Psi}_{13} = \mathbf{F}(\alpha)\mathbf{B}_1'$$

$$\boldsymbol{\Psi}_{14} = \mathbf{C}_1' + \mathbf{K}(\alpha)'\mathbf{D}_{12}'$$

$$\boldsymbol{\Psi}_{15} = \mathbf{F}(\alpha)\mathbf{B}_2 + \mathbf{C}_2'\mathbf{J}(\alpha)' - \mathbf{K}(\alpha)'\mathbf{H}'$$

Proof: Since the whole procedure is somehow extensive, here it is depicted only the final steps. The proof of this theorem utilizes a variation of the Finsler Lemma, Skelton et al. (1998). It is possible to demonstrate that solving the problem in Eq. (17) also accomplish the conditions in Eq. (18).

$$\begin{bmatrix} \boldsymbol{\Psi}_{K11} & \mathbf{P}(\alpha)\mathbf{B}_1 \\ \mathbf{B}_1'\mathbf{P}(\alpha) & -\mu\mathbf{I} \end{bmatrix} < \mathbf{0} \qquad \begin{bmatrix} \boldsymbol{\Psi}_{L11} & \mathbf{P}(\alpha)\mathbf{B}_1 \\ \mathbf{B}_1'\mathbf{P}(\alpha) & -\mu\mathbf{I} \end{bmatrix} < \mathbf{0} \qquad (18)$$

Where,

$$\boldsymbol{\Psi}_{K11} = (\mathbf{A}(\alpha)+\mathbf{B}_2\mathbf{K}(\alpha))'\mathbf{P}(\alpha)+\mathbf{P}(\alpha)(\mathbf{A}(\alpha)+\mathbf{B}_2\mathbf{K}(\alpha))+(\mathbf{C}_1+\mathbf{D}_{12}\mathbf{K}(\alpha))'+(\mathbf{C}_1+\mathbf{D}_{12}\mathbf{K}(\alpha))$$

$$\boldsymbol{\Psi}_{L11} = \left(\mathbf{A}(\alpha)+\mathbf{B}_2\mathbf{H}^{-1}\mathbf{J}(\alpha)\mathbf{C}_2\right)\mathbf{P}(\alpha)+\mathbf{P}(\alpha)\left(\mathbf{A}(\alpha)+\mathbf{B}_2\mathbf{H}^{-1}\mathbf{J}(\alpha)\mathbf{C}_2\right)+\left(\mathbf{C}_1+\mathbf{D}_{12}\mathbf{H}^{-1}\mathbf{J}(\alpha)\right)+\left(\mathbf{C}_1+\mathbf{D}_{12}\mathbf{H}^{-1}\mathbf{J}(\alpha)\right)$$

The first LMI of Eq. (18) is the H_∞ Bounded Real Lemma for the uncertain state-feedback ($\mathbf{K}(\alpha)$) closed-loop, Oliveira et al. (2004), and the second is the equivalent for output-feedback control ($\mathbf{L}(\alpha)=\mathbf{H}^{-1}\mathbf{J}(\alpha)$).

■

Alone, the conditions of the second stage, Eq. (17), describe a bilinear matrices inequality due to the terms with two variable product ($\mathbf{K}(\alpha)$ and $\mathbf{F}(\alpha)$). However, by utilizing the gain from the first stage as input for the second stage it becomes an LMI problem, which can be easily solved with optimization methods, and $\mathbf{K}(\alpha)$ behaves as a slack variable.

The formulation of the problem in *Matlab*® utilized the LMI modeling toolboxes *ROLMIP* (Agulhari et al., 2012b) and *YALMIP* (Löfberg, 2004), which allows to easily change the degrees of variables when required. To actually solve the LMI, the semi-definite solver *SDPT3 v.4* (Toh et al., 1999) is used. And the simulation of the system time response used *Simulink*®.

RESULTS

Model approximations

Least square method is applied to obtain polynomial approximation, in this case a second order, for the bearings stiffness and damping parameters according to the rotational speed, numerically modeled by Machado and Cavalca (2009). Figure 3 illustrates the approximation plot of bearing 1 coefficients (very similar to bearing 2). The error and its standard deviation are described in Table 1. In general, the approximations show small errors, except for the cross coupled damping parameters (Cyz and Czy) at lower frequencies. It's important to highlight that the coefficients approximation, shown in Figure 3, are suitable in the frequency range from 10 to 55Hz. Figure 4 shows two singular values plots, one for the rotor at 10Hz (Figure 4(a)), and near the instability, at 45Hz (Figure 4(b)). The black line (G) represents the full original system, and the red line (Gr) the reduced polynomial approximated system. Observing Figure 4, it is possible to notice that the previously cited parametrical errors have small impact over the system dynamic, and moreover, the Guyan approximation provided an acceptable model to frequencies up to 1000Hz.

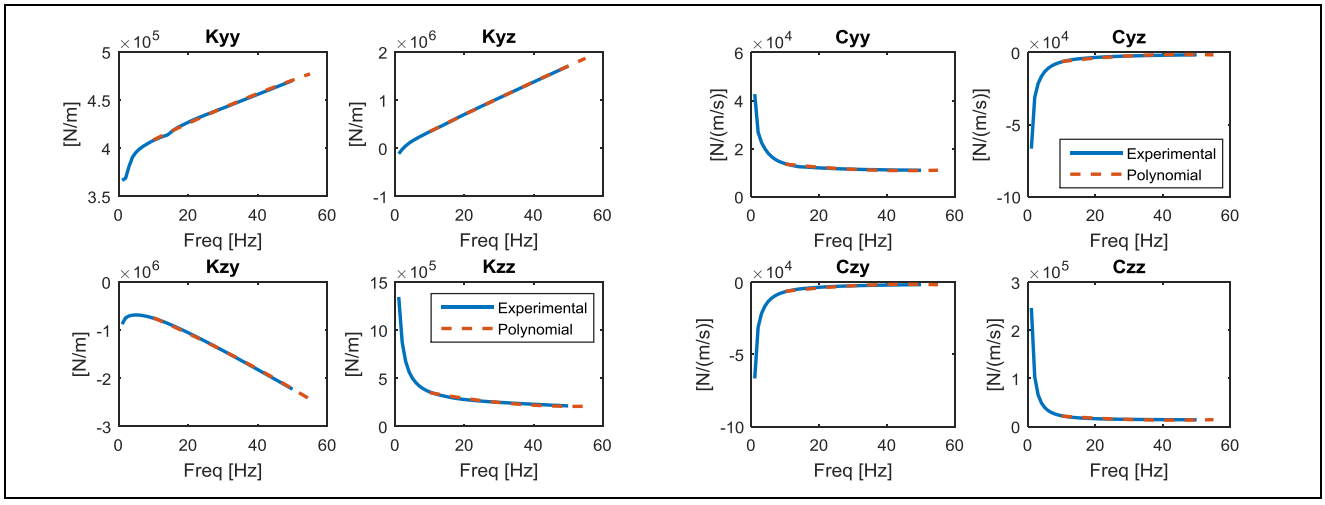

Figure 3 – Comparison between bearing 1 equivalent coefficients and polynomial approximations.

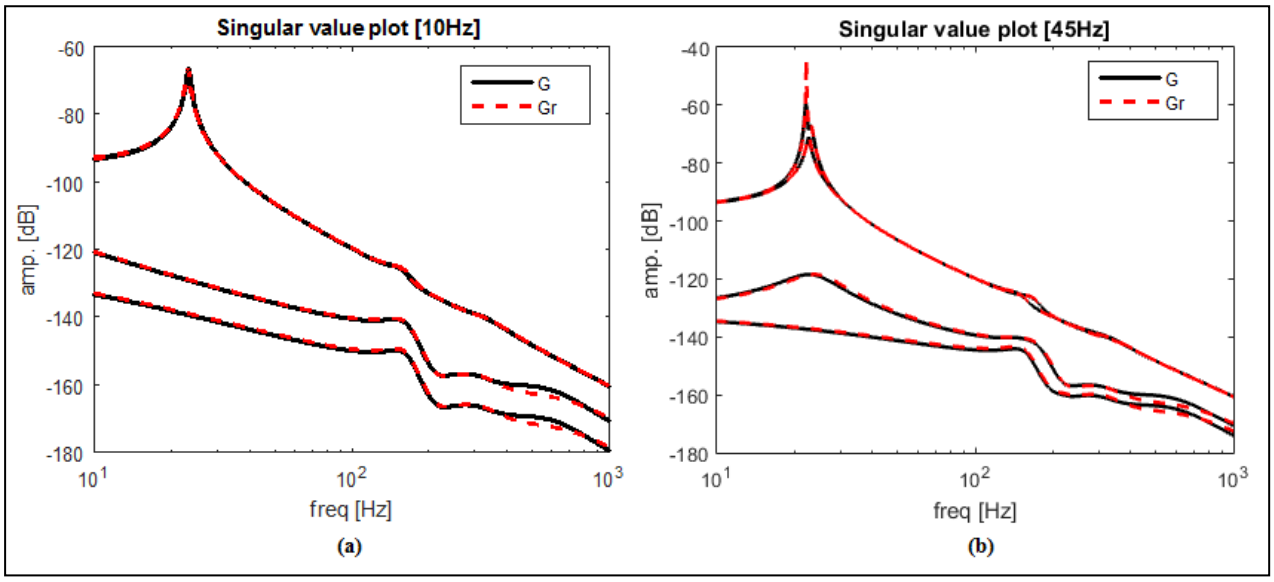

Figure 4 – Singular values comparison between original (black) and reduced (red) systems: (a) rotational speed: 10 Hz; (b) rotational speed: 45 Hz.

Table 1 – Errors between bearings equivalent coefficients and polynomial approximations.

	Coefficients	Error Mean [%]	Standard Deviation [%]
Bearing 1	Kyy	0.170	0.182
	Kyz	0.298	0.372
	Kzy	0.766	0.907
	Kzz	2.888	3.191
	Cyy	1.751	2.006
	Cyz	12.432	13.587
	Czy	12.427	13.583
	Czz	4.736	5.261
Bearing 2	Kyy	0.135	0.169
	Kyz	0.266	0.303
	Kzy	0.923	1.080
	Kzz	3.304	3.638
	Cyy	2.686	3.039
	Cyz	13.897	15.153
	Czy	13.899	15.157
	Czz	6.540	7.236

Stability and frequency response analysis

The performance analysis is represented here by a frequency response *approximation* for MIMO systems using the systems singular values. From 10Hz up to 55Hz, for each 0.1Hz interval, an equivalent full rotor model (168 states) was generated, with the original bearings parameters, and its eigenvalues and singular value were analyzed at the respective frequency with open-loop (G) and closed-loops (L0, L1, L2, Hinf and Kmu). This way, the upper curves of the pairs in the diagrams represent the expected worst case amplification of the disc displacement due to the unbalance force, and they are interrupted when instability is reached. Figure 5 compares the best gain-scheduled results obtained by the two-stage methods for constant (L0), linear (L1, Eq. (19)) and quadratic (L2) L(Ω) gain. Note that all the controllers managed to guarantee stability for the whole frequency range and attenuate the peak response, while in open-loop (G) the rotor becomes instable at about 47.3Hz because of the oil-whip effect. It can also be remarked that increasing the degree of the control gain to 2 didn't have considerable performance improvement over 1 degree, only requiring more computational effort to solve the problem.

$$\mathbf{L_1} = 10^6 \left(\begin{bmatrix} 1.515 & 0.904 & -0.403 & 0.9737 \\ -1.723 & 1.927 & -0.843 & -0.405 \end{bmatrix} \alpha + \begin{bmatrix} 0.949 & 0.735 & 0.064 & 0.489 \\ -0.867 & 2.259 & -0.971 & -0.472 \end{bmatrix} (1-\alpha) \right) \tag{19}$$

Where,

$$\alpha = \frac{(\Omega - 10)}{(55 - 10)}$$

Assuming L1 the best option, it was then compared to H_∞ (Hinf) and μ-synthesis (Kmu) controllers designed utilizing *hinfsyn* and *dksyn* functions from *Matlab Robust Control Toobox™*. Figure 6 shows that H_∞ attained 21,46% of the original peak, smaller than L1 (35,94%), however the H_∞ controller couldn't stabilize the system above 42.1Hz. While, the μ-synthesis controller assured stability in detriment of a larger peak response (125,78%). Since verifying the stability in discrete intervals, accurately speaking, can skip unstable condition, one can also check the stability via Lyapunov condition (Theorem 1). Choosing a first degree $\mathbf{P}(\alpha)$, the criterion was fulfilled for all closed-loops with gain-scheduled and μ-synthesis controllers, and, as expected, not for the open-loop (G) and H_∞ since both are unstable at some point within the considered rotational speed range. This analysis was made considering the reduced plant due to computational constraint.

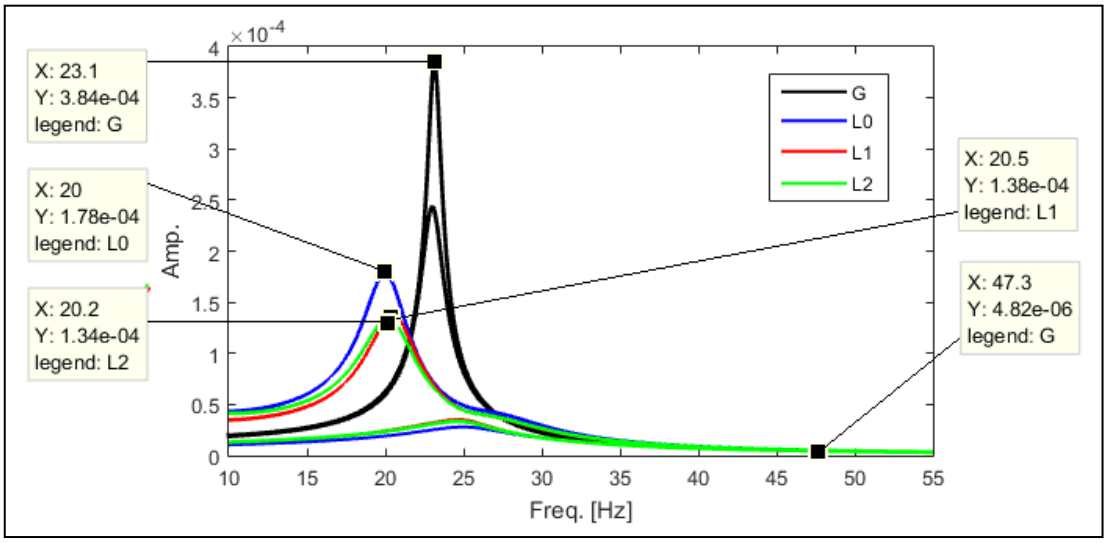

Figure 5 – Frequency response of the closed-loops with different degree controllers.

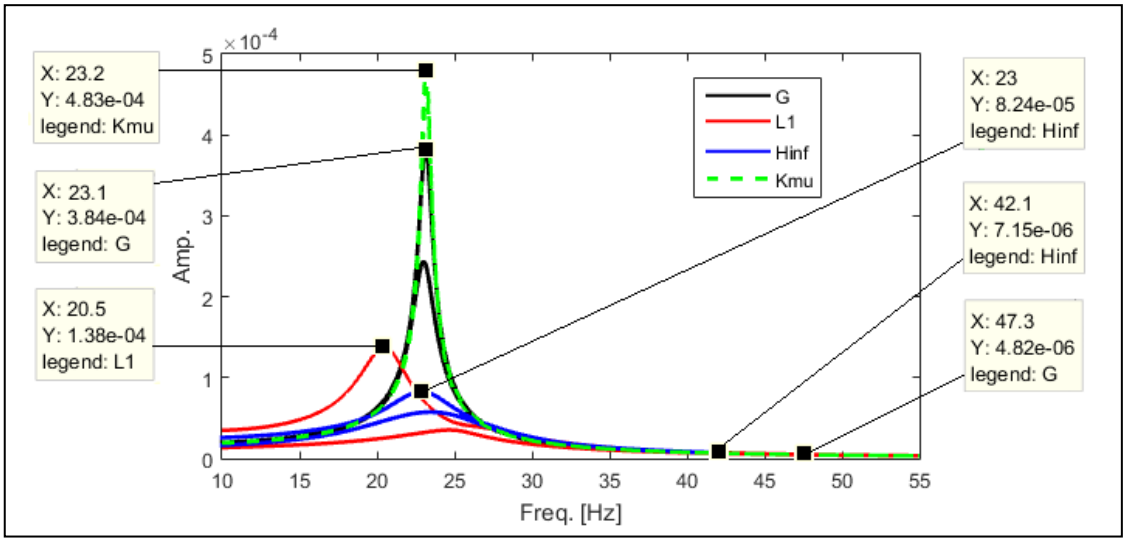

Figure 6 – Frequency response of the closed-loops with gain-schedule, H_∞ and μ-synthesis controllers.

Unbalance time response

The frequency response approximation can be verified by simulations of the system time response to the unbalance force at different frequencies. Figure 7 and Figure 8 respectively show the simulation of the disc displacement behavior in open and closed-loop at the critical speed (23Hz) and above the stability limit (55Hz). As predicted before, in Figure 6 analysis, the μ-Synthesis controller amplified the response near the critical speed, while the L1 gain-scheduled controller presented the best performance. Figure 8 only displays the L1 and Kmu curves since the open-loop and the H_∞ closed-loop were both unstable in this condition.

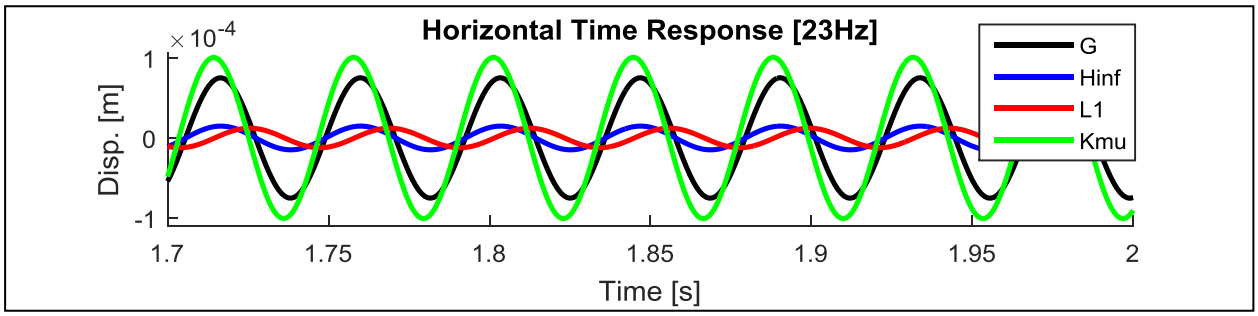

Figure 7. – Rotor response to the unbalance force [23Hz]

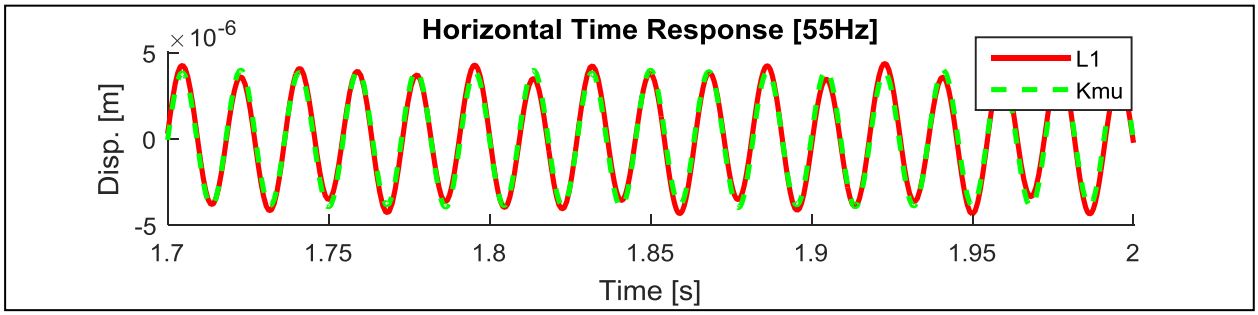

Figure 8. – Rotor response to the unbalance force [55Hz]

CONCLUSION

In this paper, gain-scheduled H_∞ controllers of different degrees were successfully designed and simulated utilizing the two-stage technique based on Lyapunov stability, and its potential for stabilizing rotating machinery systems was demonstrated. The resultant controller presented high performance, a rather simple structure when compared to other methods, and assured stability. In addition, this technique still has more to offer when it comes to unmonitored uncertainties, which can be extremely useful for practical applications. On the other hand, its synthesis takes a significant amount of computational effort to solve the LMI problems and, for this reason, when applied to FEM systems, reduction methods probably will be necessary. Another issue is that the formulation doesn't assure optimum solution. However, an alternative can be utilizing search algorithms to find sub-optimum results.

ACKNOWLEDGMENTS

The authors would like to thank the funding support by CNPq (Conselho Nacional de Desenvolvimento Científico e Tecnológico) (grants #131882/2016-3 and #302554/2015-7), and grants #2016/13059-1 and #2015/20363-6, São Paulo Research Foundation (FAPESP).

REFERENCES

Agulhari, C. M., Oliveira, R. C. L. F. and Peres, P. L. D., LMI Relaxations for Reduced-Order Robust H_∞ Control of Continuous-Time Uncertain Linear Systems, IEEE Transactions on Automatic Control, v. 57, 2012a, pp. 1532-1537.

Agulhari, C. M., Oliveira, R. C. L. F. and Peres, P. L. D., Robust LMI Parser: A Computational Package to Construct LMI Conditions for uncertain systems, Proceedings of XIX Brazilian Conference of Automation, 2012b, pp. 2298-2305.

Balini, H. M. N. K., Scherer, C. W. and Witte, J. Performance Enhancement for AMB Systems Using Unstable H∞ Controllers, IEEE Transactions on Control Systems Technology, v. 19, 2011, pp. 1479-1492.

Bernussou, J., Peres, P. L. D.and Geromel, J. C., A Linear Programming Oriented Procedure for Quadratic Stabilization of Uncertain Systems, Systems & Control Letters, 1989, pp 65-72.

Fittro, R. L. and Knospe, C. R., Rotor Compliance Minimization via μ-Control of Active Magnetic Bearings. IEEE Transactions on Control Systems Technology, v. 10, 2002, pp 238-249.

Fujita, M., Hatake, K. and Matsumura, F. Loop shaping based robust control of a magnetic bearing. IEEE Control System Magazine, v. 13, 1993, pp. 57–65.

Guyan, R. J. Reduction of Stiffness and Mass Matrices, AIAA Journal, v. 3, 1965, pp 380.

Lu, B., Choi, H. and Buckner, G. LPV control design and experimental implementation for a magnetic bearing system, IEEE Proceedings of American Control Conference, 2006, pp. 4570–4575.

Löfberg, J., YALMIP: A Tool for Modeling and Optimization in MATLAB, Proceedings of the CACSD Conference, Taipei, 2004.

Machado, T. H. and Cavalca, K. L. Evaluation of Dynamic Coefficients of Fluid Journal Bearings with Different Geometries, Proceedings of 21st COBEM, ABCM, 2009.

Maslen, E. and Schweitzer, G. Magnetic Bearings, University of Virginia, Springer, 2009.

Matsumura F., Namerikawa, T., Hagiwara and K., Fujita, M, Application of gain scheduling H∞ robust controllers to a magnetic bearing. IEEE Transactions on Control Systems Technology, vol. 4, no. 5, 1996, pp. 484-493.

Mendes, R. U., Ferreira, L. O. S. and Cavalca, K. L., Analysis of a complete model of rotating machinery excited by magnetic actuator system. Proceedings of the Institution of Mechanical Engineers C, v. 227, n. 1, pp. 48-64, 2013.

Mendes, R. U. Validação Experimental de Modelo para Identificação de Parâmetros de Falha por Desgaste de Mancais Lubrificados, Dissertação de Doutorado, Faculdade de Engenharia Mecânica, Universidade Estadual de Campinas, 2016, 153p.

Nelson, H. D., Mcvaugh, J. M., The Dynamics of Rotor-Bearing Systems Using Finite Elements, Journal of Engineering for Industry, p.593-600, May 1976.

Nonami, K. and Ito, T., μ Synthesis of Flexible Rotor-Magnetic Bearing Systems, IEEE Transactions on Control Systems Technology, v. 4, 1996, pp. 503–512.

Oliveira, P. J., Oliveira, R. C. L. F., Leite, V. J. S., Montagner, V. F. and Peres, P. L. D., H∞ Guaranteed Cost Computational by Means of Parameter-Dependent Lyapunov Functions, Elservier Automatica, 2004, pp. 1053-1061.

Ramos, D. C. W. and Peres, P. L. D., An LMI Approach to Compute Robust Stability Domains for Uncertain Linear Systems, Proceedings of the American Control Conference, 2001.

Riemann, B., Perini, E. A., Cavalca, K. L., Castro, H. F. and Rinderknecht, S., Oil Whip Instability Control Using μ-Synthesis Technique on a Magnetic Actuator, Elsevier Journal of Sound and Vibration, 2013a, pp. 654-673.

Riemann, B., Sehr, M. A., Schittenhelm, R. S. and Rinderknecht S., Robust Control of Flexible High-Speed Rotors via Mixed Uncertainties, IEEE Proceedings of the 12th European Control Conference, 2013b, pp 2343-2350.

Scherer, C. W., LMI Relaxations in Robust Control, European Journal of Control, 2006, pp. 3-29.

Siqueira, A. A. G., Nicoletti, R., Norrick, N., Cavalca, K. L., Castro, H. F., Bauer, J. and Dohnal, F., Linear Parameters Varying Control Desing for Rotating Systems Supported by Journal Bearings, Elsevier Journal of Sound and Vibration, 2012, pp. 2220-22232.

Skelton, R. E., Iwasaki, T. and Grigoriadis, K., A Unified Algebraic Approach to Linear Control Design, Taylor & Francis, London, 1998, ch. 2.

Toh, K. C., Todd, M. J. and Tutuncu, R. H., SDPT3 - a Matlab Software Package for Semidefinite Programming. Optimization Methods and Software, 1999, pp. 545-581.

Wu, F. Switching LPV Control Design for Magnetic Bearing Systems, IEEE International Conference on Control Applications, 2001, pp. 41–46.

Wu, M. F., Aplicação de Controlador LPV no Controle Ativo de Rotores, Trabalho de Graduação II, Faculdade de Engenharia Mecânica, Universidade Estadual de Campinas, 2015a, 89p.

Wu, M. F., Mendes, R. U. and Cavalca, K. L., Comparative Study of Rotor Active Vibration Control Performance Using H∞ and μ-Synthesis, Proceedings of 23st COBEM, ABCM, 2015b.

RESPONSIBILITY NOTICE

The authors are the only responsible for the material included in this paper.